

# Laser-Assisted Synthesis of Au–Ag Alloy Nanoparticles in Solution

Zhangquan Peng,<sup>†</sup> Bernd Spliethoff,<sup>‡</sup> Bernd Tesche,<sup>‡</sup> Thomas Walther,<sup>§</sup> and Karl Kleinermanns<sup>\*,†</sup>

*Institut für Physikalische Chemie, Heinrich-Heine-Universität Düsseldorf, 40225 Düsseldorf, Germany, Max-Planck-Institut für Kohlenforschung, Kaiser-Wilhelm-Platz 1, 45470 Mülheim an der Ruhr, Germany, and Center of Advanced European Studies and Research, Ludwig-Erhard-Allee 2, 53175 Bonn, Germany*

*Received: November 18, 2005; In Final Form: December 20, 2005*

By using laser-induced heating, we prepared Au–Ag nanoalloys via three different procedures: (i) mixture of Au nanoparticles and  $\text{Ag}^+$  ions irradiated by a 532 nm laser, (ii) mixture of Au and Ag nanoparticles irradiated by a 532 nm laser, and (iii) mixture of Au and Ag nanoparticles irradiated by a 355 nm laser. Procedure i is advantageous for the production of spherical alloy nanoparticles; in procedures ii and iii, nanoalloys with a sintered structure have been obtained. The morphology of the obtained nanoalloys depends not only on the laser wavelength but also on the concentration of nanoparticles in the initial mixture. When the total concentration of Ag and Au nanoparticles in the mixture is increased, large-scale interlinked networks have been observed upon laser irradiation. It is expected that this selective heating strategy can be extended to prepare other bi- or multi-metallic nanoalloys.

## 1. Introduction

Bimetallic nanoparticles, either as alloys or as core–shell structures, are attractive materials because of their composition-dependent optical and catalytic properties.<sup>1,2</sup> Nanostructures from Au, Ag, and their combinations have been the focus of extensive research efforts due to their unique surface plasmon absorption in the visible spectral region.<sup>3</sup> One important observation of Au–Ag bimetallic systems is that alloy and core–shell nanoparticles often show different optical properties, although the composition of Au and Ag within the nanostructures is the same.<sup>4</sup> Au–Ag core–shell nanoparticles in the form of  $\text{Au}_{\text{core}}\text{Ag}_{\text{shell}}$  or  $\text{Ag}_{\text{core}}\text{Au}_{\text{shell}}$  can be synthesized by successive reduction of one metal ion over the core of the other.<sup>5</sup> Their optical properties depend critically on the relative composition/thickness of the core and shell.<sup>6</sup> If the shell is not very dense and thick, the surface plasmon of the core can effectively interact with the electromagnetic field so that the surface plasmon absorption of the core particles can be observed. In this case, two distinct surface plasmon (SP) absorption peaks around 400 and 520 nm (corresponding to pure Ag and Au nanoparticles, respectively) were observed.<sup>5,6a</sup> In some other cases, only the Ag–SP peak was observed for Au–Ag core–shell nanoparticles, demonstrating their relative composition/thickness dependent optical properties.<sup>6b,c</sup> In contrast, Au–Ag alloy nanoparticles show a single, composition-sensitive absorption band located at an intermediate position between pure Au and Ag nanoparticle surface plasmon peaks.<sup>4,7</sup> For the preparation of Au–Ag alloy nanoparticles, evaporation of bulk alloy<sup>8a</sup> and co-reduction of the metal salts<sup>8b</sup> have been reported. More recently, a physical method called “laser ablation” has been developed to prepare metal nanoparticles in solution.<sup>9</sup> This laser-based method also demonstrated its great potentials for the preparation

of metal alloy nanoparticles. For example, Kim et al.<sup>10</sup> reported that Au–Ag alloy nanoparticles can be produced by pulsed laser irradiation of bulk alloy metals in water and that the obtained alloy nanoparticles preserve the stoichiometry of the target metals. Chen and Yeh<sup>7</sup> reported that alloy nanoparticles could be produced by laser irradiation of mixtures consisting of Au and Ag nanoparticles. Additionally, Hodak et al.<sup>4a</sup> showed that nanosecond or picosecond laser-induced heating can melt  $\text{Au}_{\text{core}}\text{Ag}_{\text{shell}}$  nanoparticles into homogeneous alloyed nanoparticles. Similar results have also been reported by Girault and co-workers.<sup>4b</sup> The transformation comes from the selective heating caused by resonant electronic excitation of the Au core nanoparticles by a 532 nm laser because its energy is in the vicinity of the absorption maximum of Au nanoparticles centered at around 520 nm. It has been theoretically and experimentally demonstrated that if nanoparticles possess a strong absorption band whose energy coincides with the photon energy of a laser, the nanoparticles can selectively be heated above their melting point into related liquid systems.<sup>11</sup>

In this paper, we have attempted to take advantage of this localized heating process to prepare Au–Ag alloys with nanoscale structures. Three different procedures have been used to obtain Au–Ag nanoalloys: (i) a mixture of Au nanoparticles and  $\text{Ag}^+$  ions was irradiated by a 532 nm laser, (ii) a mixture of Au and Ag nanoparticles was irradiated by a 532 nm laser, and (iii) a mixture of Au and Ag nanoparticles was irradiated by a 355 nm laser. Using electron microscopy and optical absorption spectroscopy, a comparative investigation of morphology, composition, and formation mechanism of different nanoalloys was performed.

## 2. Experimental Section

Gold(III) chloride trihydrate ( $\text{HAuCl}_4 \cdot 3\text{H}_2\text{O}$ , 99.9%), silver nitrate ( $\text{AgNO}_3$ , 99.0%), and sodium citrate dihydrate (99%) were purchased from Aldrich and used as received. Au nanoparticles with an average diameter of  $21 \pm 4$  nm were prepared by adding  $\text{HAuCl}_4 \cdot 3\text{H}_2\text{O}$  (20 mg) to a vigorously

\* Corresponding author. Fax: +49-221-8115195. E-mail: kleinermanns@uni-duesseldorf.de.

<sup>†</sup> Heinrich-Heine-Universität Düsseldorf.

<sup>‡</sup> Max-Planck-Institut für Kohlenforschung.

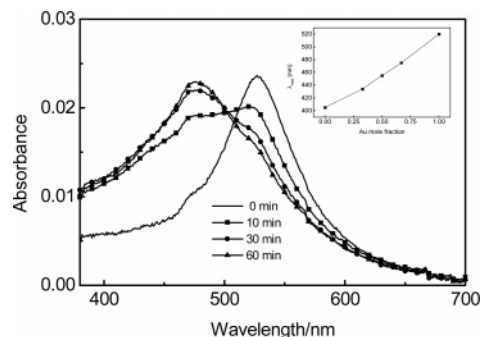
<sup>§</sup> Center of Advanced European Studies and Research.

stirred solution of sodium citrate (60 mg) in boiling water (250 mL). The solution was stirred under reflux for additional 15 min before being allowed to cool. Ag nanoparticles were synthesized in a similar way, and larger size distributions (average diameters of  $30 \pm 6$  nm) with different morphologies including spherical particles, rods, and triangles have been observed. The pH values of the parent Au and Ag colloidal solutions are 5.3 and 5.6, respectively.

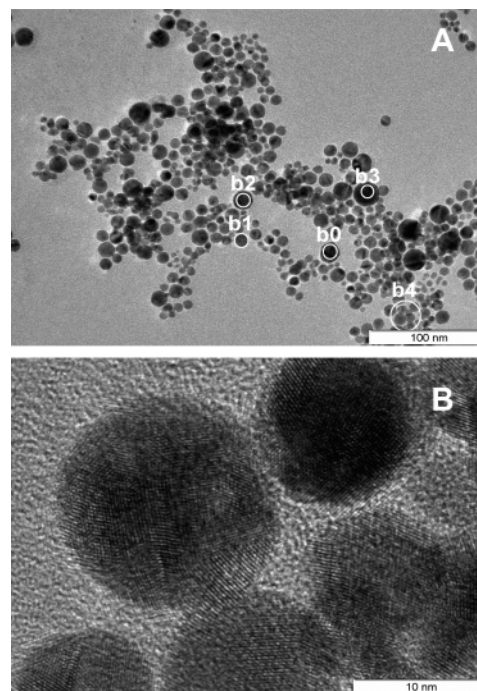
A pulsed Nd:YAG laser (Quanta Ray INDI series, Spectra-Physics, Mountain View, CA) was used to irradiate the colloidal solution at 532 or 355 nm. The energy fluence per pulse is  $130 \text{ mJ/cm}^2$  (at 532 nm) or  $150 \text{ mJ/cm}^2$  (at 355 nm) with a pulse length of 6 ns, 8 mm beam diameter, and a repetition rate of 10 Hz. Optical absorption spectra of the colloidal solution were recorded by using a Cary 300 UV-vis spectrophotometer. Quartz micro-cells (Hellma 105-QS) containing different initial mixtures of interest have been used for both the laser irradiation and the UV-vis measurement. Size and shape of the Au and Ag nanoparticles and their alloys were investigated by bright-field transmission electron microscopy (TEM), and their chemical composition was investigated by energy-dispersive X-ray (EDX) microanalysis in a Hitachi HF2000 electron microscope operated at an acceleration voltage of 200 kV and equipped with a Noran HP-Si X-ray detector. Further chemical studies were conducted by EDX mapping in scanning TEM (STEM) mode with a 0.8 nm electron beam in a Zeiss Libra 200FE electron microscope equipped with an Oxford Instruments Si(Li) X-ray detector. TEM samples were prepared by mounting a droplet of the colloidal solution of interest on a carbon-coated copper grid (Cu-400CK, Pacific Grid-Tech) and allowing it to dry in air.

### 3. Results and Discussion

**3.1. Au–Ag Nanoalloys Formed by 532 nm Laser Excitation of Mixtures of Au Nanoparticles and  $\text{Ag}^+$  Ions.** The Au nanoparticles obtained by citrate reduction have an average diameter of 21 nm and a characteristic surface plasmon absorption at about 520 nm.<sup>12</sup> The concentration of Au atoms in the form of nanoparticles in the colloidal solution is estimated to be 0.16 mM. An initial estimate indicates that the concentration of  $\text{Cl}^-$  ions ( $\sim 0.64 \text{ mM}$ ) existing in the Au colloidal solution is too high to ensure complete solubility of  $\text{Ag}^+$  ions from our stock  $\text{AgNO}_3$  solution (0.16 mM). For this reason, both Au colloids and  $\text{Ag}^+$  ions used in procedure (i) are diluted by a factor of 50 to lower the solubility product to  $4.1 \times 10^{-11}$ , safely below the  $K_{\text{sp}}$  of  $\text{AgCl(s)}$ ,  $1.8 \times 10^{-10}$ . The solid curve in Figure 1(0 min) shows the UV-vis spectrum of a mixed solution of Au colloids and  $\text{Ag}^+$  ions with a molar ratio of 2:1. Under the conditions of low concentrations of  $\text{Cl}^-$  and  $\text{Ag}^+$  ions, the Au nanoparticles are stable and dispersed in the mixed solution, and no ionic strength-induced aggregation takes place. After laser irradiation at 532 nm, the characteristic plasmon peak of the Au nanoparticles gradually shifts to the blue, diminishes, and finally becomes almost unobservable. Instead, a new absorption band centered at 475 nm is formed and intensified. From these spectral changes, it can be inferred that  $\text{Ag}^+$  ions are reduced on the surface of laser-heated Au nanoparticles and that the formed bimetallic structures are simultaneously melted to Au–Ag alloys. Without alloying, the Au nanoparticles with a diameter of  $\sim 21$  nm would give a sharp plasmon peak at about 520 nm in the absorption spectrum. This inference is actually proven by the electron micrographs of the products obtained after laser irradiation as shown in Figure 2, where selected nanoparticles have been analyzed by energy-dispersive



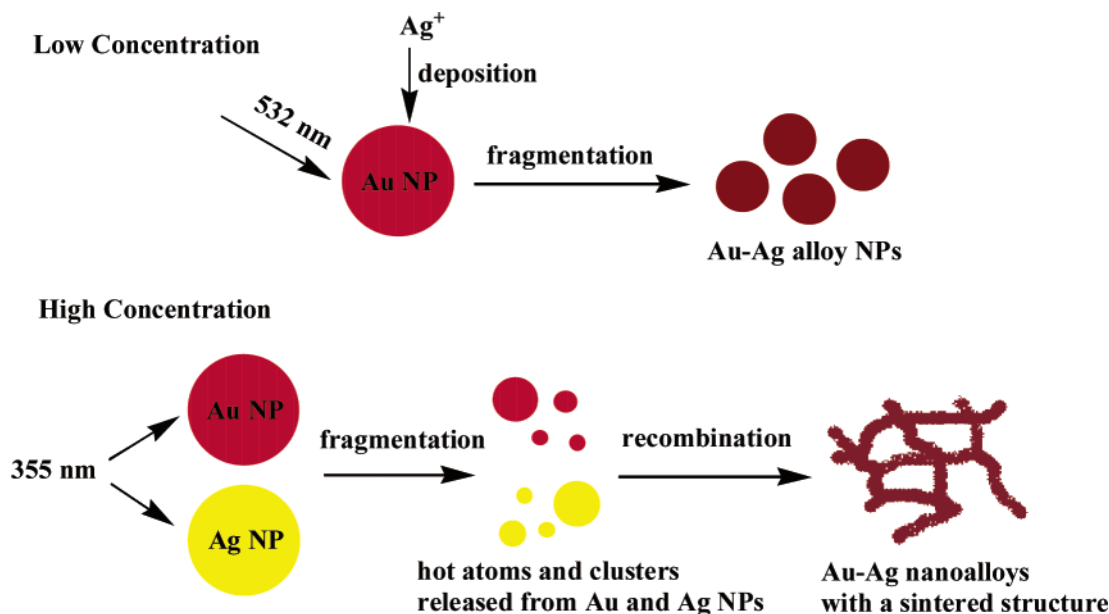
**Figure 1.** Optical absorption spectra of a mixed solution of Au nanoparticles and  $\text{Ag}^+$  ions (molar ratio 2:1) at various irradiation times using a pulsed 532 nm laser with a fluence of  $130 \text{ mJ pulse}^{-1} \text{ cm}^{-2}$ . Inset: plot of the wavelength corresponding to the maximum absorbance for Au–Ag alloy nanoparticles obtained from initial mixtures with varying mole fractions of Au nanoparticles and  $\text{Ag}^+$  ions.



**Figure 2.** (A) TEM bright-field image of Au–Ag alloy nanoparticles produced by laser irradiation of a mixed solution of Au nanoparticles and  $\text{Ag}^+$  ions (molar ratio 2:1) for 60 min. The EDX microanalysis demonstrated that nanoparticles marked as b0 and b3 are pure Au nanoparticles, while the other selected particles are alloy nanoparticles with composition (Au:Ag) of 2.4 (b1) and 3.6 (b2). The nanoparticle ensemble (b4) has a Au:Ag ratio of 2.4. (B) High-resolution TEM image of the Au–Ag alloy nanoparticles.

X-ray (EDX) microanalysis. The EDX analysis of different nanoparticles shows that most of the nanoparticles with diameters less than 10 nm (smaller than the 21 nm parent Au nanoparticles) are alloy nanoparticles. Few large nanoparticles with a size consistent with that of the parent Au nanoparticles are observed. They consist of pure Au and are most probably the unexcited parent Au nanoparticles.

Under irradiation with an intense pulsed laser at 532 nm, a parent Au nanoparticle in the solution will absorb multiple-photons during a single laser pulse and will be heated to its boiling point in a few picoseconds via electron–phonon interactions.<sup>11</sup> These hot Au nanoparticles may be fragmented into smaller nanoparticles by releasing atoms and clusters provided that the energy of the laser pulse is high enough. Besides, Au nanoparticles will be efficiently ionized via ejection

**SCHEME 1: Proposed Mechanism for the Formation of Au–Ag Nanoalloys under Different Experimental Conditions**

of electrons, and the charge density produced may be sufficient to cause explosive repulsion.<sup>13</sup> Both the elevated temperature of the parent Au nanoparticles and the ejected electrons are advantageous for the reduction of Ag<sup>+</sup> ions. During a single laser pulse, Ag<sup>+</sup> ions in the close vicinity of the Au nanoparticles are promptly reduced by citrate at the achieved elevated temperature or possibly by the ejected electrons. The reduced Ag is simultaneously melted by heat transfer from the parent Au nanoparticles, leading to diffusion of the atoms and formation of Au–Ag alloy nanoparticles. Because of the similarity between Au and Ag, particularly their very similar lattice constants (Au, 4.0786 Å; Ag, 4.0862 Å), complete miscibility of Au and Ag at any composition can be obtained in the bulk, as well as on the nanometer scale.<sup>14</sup> Hence, the Au nanoparticles serve both as the nucleus site for the deposition of Ag<sup>+</sup> ions and as the heat source for formation of alloys. After each laser pulse, the internal energy is transferred fast enough to the solution so that the nanoparticles cool and stabilize before the next laser pulse arrives. Neither pure Ag nanoparticles nor Au–Ag core–shell structures were observed in solution after 532 nm laser irradiation as seen from the absence of any plasmon band absorption around 400 nm and from our EDX microanalysis. Optical absorption spectra of alloy nanoparticles obtained from the initial solutions with different Au:Ag molar ratios show that the new absorption band shifts blue as the molar fraction of Ag increases (see Figure 1, inset). Hence, by simply varying the Ag<sup>+</sup> content of the solution, the absorption wavelength of the laser-prepared nanoalloys can be tuned over more than 100 nm. Scheme 1 shows the possible formation process of the Au–Ag alloy nanoparticles.

**3.2. Au–Ag Nanoalloys Formed by Laser Excitation of Mixtures of Au and Ag Nanoparticles at 532 and 355 nm, Respectively.** We have demonstrated that laser-induced heating can promote reduction and deposition of Ag<sup>+</sup> ions and alloying of Au and Ag. Laser-induced heating may also alloy Ag and Au when the Ag source is in the form of dispersed nanoparticles. Figure 3 shows the optical absorption spectra of a mixed Au (0.16 mM) and Ag (0.16 mM) nanoparticle solution before and after laser irradiation at 532 nm. Before exposure to laser light, two distinct absorbance maxima at 406 and 520 nm, corresponding to Ag and Au nanoparticle surface plasmon bands, respectively, indicate isolated Ag and Au nanoparticles in the

mixed solution (Figure 3, inset). For solutions exposed to laser irradiation at 532 nm, the absorption spectra change as the irradiation time is increased. The Au surface plasmon absorption intensity decreases and shifts to the blue, while the Ag surface plasmon absorption intensity increases without obvious spectral shift. This variation in UV–vis spectra clearly implies changes in the colloidal properties. Further irradiation leads to a new absorption shoulder at 460 nm, located at an intermediate position between the Au and Ag nanoparticle surface plasmon bands. This new absorption band is likely due to the formation of a Au–Ag alloy.<sup>8b</sup> Otherwise, only two plasmon absorption bands at around 400 and 520 nm would be expected if the colloids consisted of isolated previously melted Au and Ag particles or of bimetallic composites such as core–shell structures.<sup>1</sup> We observe that elimination of the Ag surface plasmon band needs very long irradiation times at 532 nm, while Chen and Yeh reported that already a short time irradiation (245 mJ pulse<sup>−1</sup>) removes the Ag plasmon band.<sup>7</sup> This difference may come from the different experimental parameters such as the laser power and the initial size (or amount) of the Au and Ag nanoparticles in the mixed solution. The size of the Ag nanoparticles in our starting solution is quite large, so that the energy absorbed by the parent Au nanoparticles may be not large enough to melt and alloy all of the Ag nanoparticles. We observed, however, that after decrease of the relative concentration of Ag nanoparticles in the starting solution (for example,

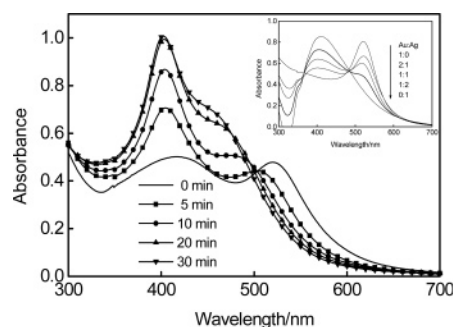


**Figure 3.** Optical absorption spectra of a mixed solution of Au and Ag nanoparticles (molar ratio 1:1) at various irradiation times using a pulsed 532 nm laser with a fluence of 130 mJ pulse<sup>−1</sup> cm<sup>−2</sup>. Inset: optical absorption spectra of Au and Ag nanoparticle mixtures in water at different molar ratios.



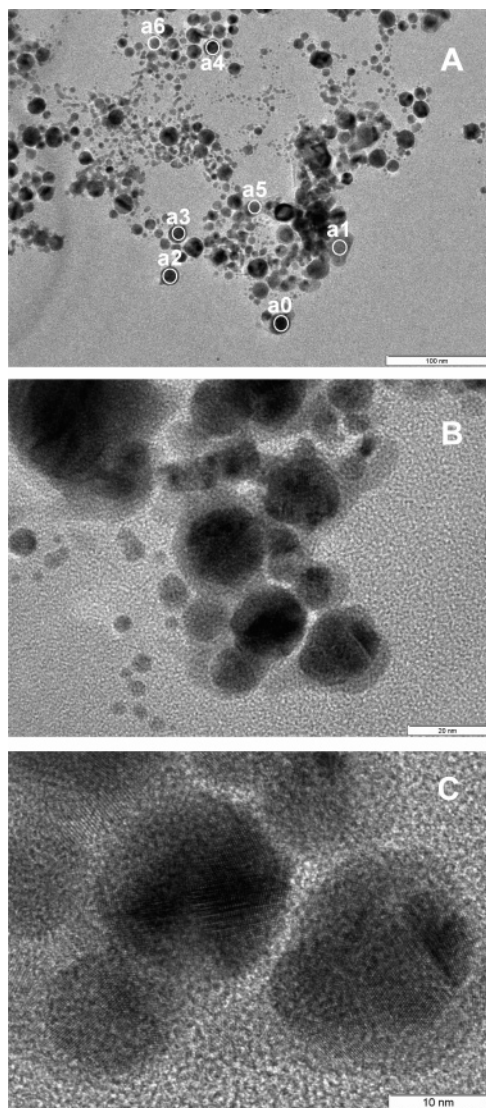


**Figure 4.** (A) TEM bright-field image of photoproducts after laser irradiation of a mixed solution of Au and Ag nanoparticles (molar ratio 1:1) for 30 min by a pulsed 532 nm laser with a fluence of  $130 \text{ mJ pulse}^{-1} \text{ cm}^{-2}$ . EDX microanalysis demonstrated that the nanoparticle marked as A1 is a pure Ag nanoparticle, while the other selected particles are alloy nanoparticles with composition (Au:Ag) of 1.8 (a0), 2.0 (a2), 1.95 (a3), 1.8 (a4), 0.37 (a5), and 0.11 (a6). (B) TEM micrograph at higher magnification where small nanoparticles and sintered structures are presented. (C) High-resolution TEM image of the Au–Ag alloy nanoparticles.

Au:Ag 5:1), the absorbance of the Ag nanoparticles could be removed by laser irradiation at 532 nm for 30 min. Figure 4 displays the TEM bright-field images of the mixed colloids (Au:Ag ratio of 1:1) after 532 nm laser irradiation for 30 min. Photofragmentation of the parent nanoparticles and some sintered structures (Figure 4B) have been observed. EDX microanalysis indicates that mainly Au–Ag alloy nanoparticles and unalloyed Ag nanoparticles were obtained after laser irradiation. Upon intense pulsed laser irradiation at 532 nm, the Au nanoparticles in the mixed colloidal solution were excited and heated to their boiling point. Some large Ag nanoparticles can also be heated because they also have a rather strong absorption at 532 nm.<sup>15</sup> It is possible that some Ag nanoparticles reach their melting (or boiling) point even before Au nanoparticles reach theirs because the melting (or boiling) point of Ag nanoparticles is lower than that of Au nanoparticles. This hypothesis is reasonable from our observation in Figure 3, where

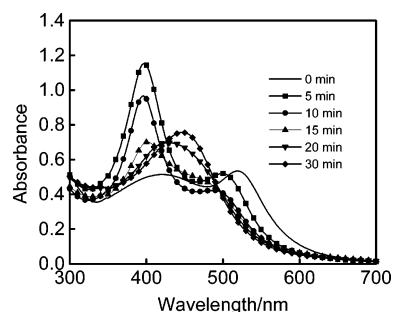


**Figure 5.** Optical absorption spectra of a mixed solution of Au and Ag nanoparticles (molar ratio 1:1) at various irradiation times using a pulsed 355 nm laser with a fluence of  $150 \text{ mJ pulse}^{-1} \text{ cm}^{-2}$ .

irradiation of the mixed colloidal solution for a short time (e.g., 5 min) has only a small effect on the plasmon band of the Au nanoparticles, but induces dramatic changes of the plasmon band of the Ag nanoparticles. From the increased absorption intensity centered at 406 nm, we can deduce that a lot of smaller Ag nanoparticles were produced. These smaller Ag nanoparticles either exist separately in the solution or are attached to other nanoparticles. Both the isolated and the attached Ag nanoparticles contribute to the absorption increase at 406 nm. When the smaller Ag nanoparticles contact heated Au nanoparticles, alloy nanoparticles may be obtained by two modes:<sup>16</sup> (i) formation of alloy nanoparticles with a larger size or a sintered structure, and (ii) explosion into smaller alloy nanoparticles depending on the energy absorbed by the nanoparticles. The morphology of the obtained Au–Ag alloy corresponding to the two modes can be observed in Figure 4.

In the physical mixture of Au and Ag particles, absorbances for Au and Ag nanoparticles at 532 nm are 0.81 and 0.23, respectively. So upon laser irradiation at 532 nm, Au nanoparticles will be more efficiently excited than Ag nanoparticles of the same size. When the colloidal mixtures are irradiated at 355 nm, both Au and Ag nanoparticles can be excited effectively because the difference in absorption coefficients for Au (0.52) and Ag (0.38) nanoparticles at 355 nm is small. Figure 5 shows the optical absorption spectra of the mixed Au and Ag colloids with molar ratio 1:1 after 355 nm laser irradiation. In the first 5 min, the Au nanoparticle surface plasmon band decreases in magnitude and slightly shifts to the blue, while the Ag plasmon band intensity increases without obvious spectral shift. Further irradiation leads to a dramatic decrease of the absorption of the Ag surface plasmon band. A new absorption peak at 448 nm is formed and intensified. This surface plasmon band can be contributed to the formation of Au–Ag alloys. Figure 6 displays the TEM image of the mixed colloids after 355 nm laser irradiation for 30 min. A few smaller nanoparticles and a lot of aggregates can be observed. EDX microanalysis indicates that both the smaller nanoparticles and the sintered structures are Au–Ag alloys. Neither pure Au nor pure Ag nanoparticles have been found by TEM. It seems that the morphology of the products obtained depends on the wavelength of laser excitation. When both Au and Ag parent particles are effectively excited in solution, formation of nanoalloys with a sintered suprastructure becomes favorable as compared to melting of the isolated nanoparticles. Besides, the morphology of the obtained Au–Ag nanoalloys also depends on the initial composition of the mixed Au and Ag colloids. For example, when the total concentration of Au (0.16 mM) and Ag (0.96 mM) nanoparticles (molar ratio Au:Ag of 1:6) in the mixed colloidal solution is increased, more sintered suprastructures (even interlinked networks) have been observed. Figure 7A shows a scanning transmission electron microscope (STEM) annular dark-field

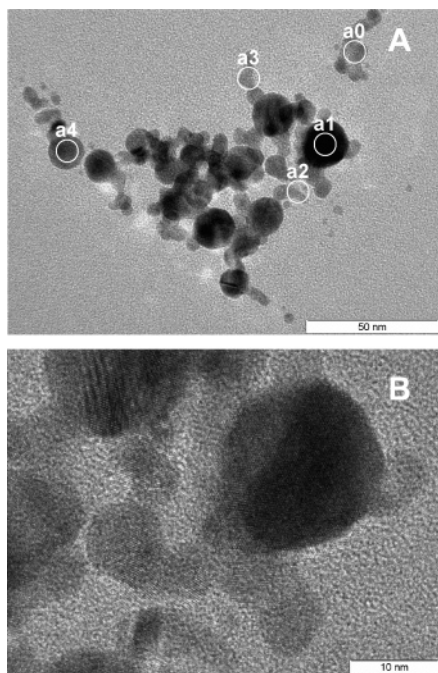


**Figure 6.** TEM bright-field image of photoproducts after laser irradiation of a mixed solution of Au and Ag nanoparticles (molar ratio 1:1) for 30 min by a pulsed 355 nm laser with a fluence of  $150 \text{ mJ pulse}^{-1} \text{ cm}^{-2}$ . EDX microanalysis demonstrated that all of the selected particles are alloy nanoparticles with composition (Au:Ag) of 0.48 (a0), 1.64 (a1), 0.59 (a2), 0.77 (a3), and 1.11 (a4). (B) High-resolution TEM image of the Au–Ag alloy nanoparticles.

image of a sample from Au and Ag mixed colloidal solutions treated with 355 nm laser irradiation for 30 min. The obtained alloy forms an interlinked network. The element distribution of Ag and Au within these nanostructures is, however, not uniform as revealed by the corresponding EDX maps of Ag K and Au L signals (Figure 7B and C), which show Au-rich structures of lateral sizes of 12 to 77 nm within a porous Ag-rich network. From the integrated X-ray intensities and appropriate  $k$ -factors, an average Au/Ag ratio of  $0.28 \pm 0.04$  is calculated where the error bar represents the difference obtained if either hard X-ray lines ( $\text{Au}_L/\text{Ag}_K$ ) or softer X-rays ( $\text{Au}_M/\text{Ag}_L$ ) are compared.

**3.3. Comparison of the Three Procedures.** In a mixture of Au nanoparticles and  $\text{Ag}^+$  ions exposed to a 532 nm laser irradiation, only Au nanoparticles can be excited. In the course of the excitation (or heating) process, the temperature of the Au nanoparticles will increase from room temperature to their melting or even boiling point depending on the energy fluence. At the same time, the  $\text{Ag}^+$  ions in the vicinity of the Au nanoparticles will be reduced and deposit on the hot Au nanoparticles. The process of alloying must take place before thermal explosion of the Au nanoparticles because a much lower temperature is necessary for the formation of a nanoscale Au–Ag alloy.<sup>14</sup> This method is very beneficial for the preparation of spherical alloy nanoparticles. For example, we can lower the power of the 532 nm laser under the energy threshold for thermal or Coulombic explosion of Au nanoparticles.<sup>16</sup> In this way, all of the reduced Ag on the parent Au nanoparticle surface will alloy with Au, leading to quite large spherical nanoparticles. Because we use the standard synthesis procedure for the preparation of Au nanoparticles, that is, citrate reduction of  $\text{AuCl}_4^-$ ,<sup>6</sup> the presence of  $\text{Cl}^-$  ions limits the concentration of Au–Ag alloy nanoparticles.

When both Au and Ag nanoparticles are effectively excited via irradiation at 355 nm, alloying becomes easy because both

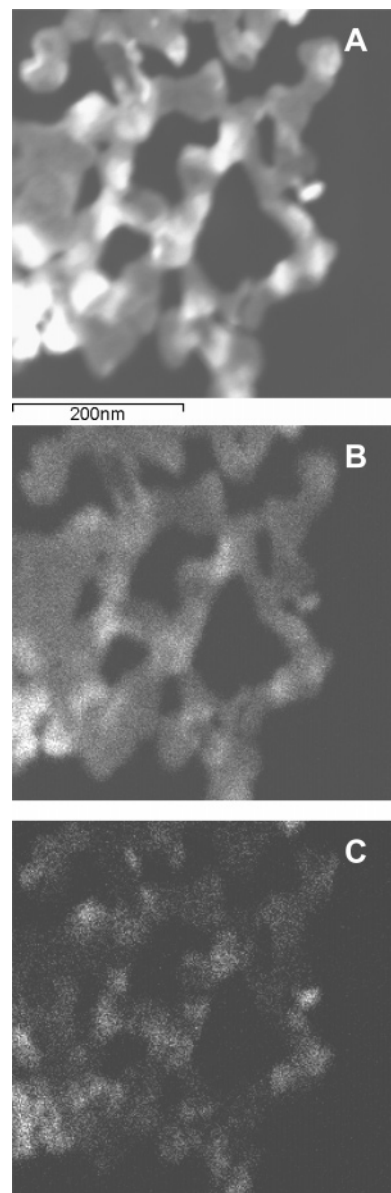


**Figure 7.** (A) STEM annular dark field image of a sample obtained from mixed colloidal solutions (Au/Ag ratio of 1:6) after 355 nm laser irradiation for 30 min. EDX maps demonstrate the spatial distribution of Ag (B) and Au (C) within the interlinked and porous nano-network.

Au and Ag nanoparticles can be heated to their respective melting/boiling points. The alloying process may take place in the following way. At 355 nm laser irradiation Au and Ag atoms and clusters will be released from the excited parent nanoparticles by Coulombic or thermal explosion mechanisms. The released atoms have a strong tendency to rapidly aggregate into small clusters on a nanosecond time scale.<sup>17</sup> Also, single atoms or small clusters might diffuse to and aggregate on the surface of preexisting nanoparticles.<sup>18</sup> In a work concerned with the mechanism of the interaction between pulsed laser light and metal nanoparticles, Kondow et al.<sup>19</sup> reported that the morphology of the photoproducts depends on the concentration of the stabilizer (in his case, Au nanoparticles stabilized by sodium dodecyl sulfate, “SDS”). In dilute SDS solution, parent Au nanoparticles and photofragments are not well stabilized by SDS molecules. When they are melted via a laser beam, they grow into network structures by encounter and coagulation. At high concentration of SDS, no aggregate structure but smaller spherical nanoparticles have been observed. Hence, the aggregation of Au nanoparticles after each laser pulse depends

on the coverage of the photoproducts by ligand molecules, and on the probability of encounters of heated Au nanoparticles with photofragments. Recent results of our group also demonstrated that photofragmentation of Au nanoparticles in the presence of strong ligands (organic thiols) leads to the formation of tiny Au nanoparticles rather than large sintered structures.<sup>20</sup> In addition to the protecting ligand, the concentration of the parent nanoparticles is also an important aspect because it determines the concentration of the photofragments. When the concentration of parent nanoparticles is low (such as in procedure i), the released photofragments also have low concentrations, so that the possibility of collisions between them decreases. These conditions are not advantageous for the formation of sintered structures but are suitable to produce spherical nanoparticles. In the case of high concentrations of the parent nanoparticles, the chance of reactive collisions between the photofragments is dramatically increased especially when both of the parent nanoparticles are excited by laser irradiation (such as in procedure iii). This recombination process between released atoms and clusters during photofragmentation of the parent nanoparticles is the basis for the nanoalloy formation (Scheme 1). Diffusion of atoms in the hot nanocomposite initially formed adds to the homogeneity of the obtained alloy.

#### 4. Conclusions

In summary, we have demonstrated that Au–Ag nanoalloys can be synthesized by 532 (or 355) nm laser irradiation of a mixed solution of Au nanoparticles and Ag ions (or nanoparticles). Some morphology control of the obtained nanoalloys could be achieved, and their formation mechanisms were discussed. The Au–Ag nanoalloys thus fabricated should show collective chemical and physical properties and may be promising for catalysis and for surface enhanced Raman spectroscopy. It is expected that this selective heating strategy can be extended to prepare other bi- or multi-metal nanoalloys.

**Acknowledgment.** Z.P. acknowledges the support from the Alexander von Humboldt Foundation.

**Supporting Information Available:** EDX microanalysis of selected nanoparticles in Figures 2, 4, and 6. This material is available free of charge via the Internet at <http://pubs.acs.org>.

#### References and Notes

- (1) Mulvaney, P. *Langmuir* **1996**, *12*, 788.
- (2) Toshima, N.; Yonezawa, T. *New J. Chem.* **1998**, *11*, 1179.
- (3) *Metal Nanoparticles: Synthesis, Characterization and Applications*; Feldheim, D. L.; Colby, A. F., Jr., Eds.; Marcel Dekker: New York, 2002.
- (4) (a) Hodak, J. H.; Henglein, A.; Giersig, M.; Hartland, G. V. *J. Phys. Chem. B* **2000**, *104*, 11708. (b) Abid, J.-P.; Girault, H. H.; Brevet, P. F. *Chem. Commun.* **2001**, 829.
- (5) (a) Ah, C. S.; Hong, S. D.; Jang, D.-J. *J. Phys. Chem. B* **2001**, *105*, 7871. (b) Cao, Y.-W.; Jin, R.; Mirkin, C. A. *J. Am. Chem. Soc.* **2001**, *123*, 7961. (c) Srnova-Sloufova, I.; Lednický, F.; Gemperle, A.; Gemperlova, J. *Langmuir* **2000**, *16*, 9928.
- (6) (a) Shipway, A. N.; Katz, E.; Willner, I. *ChemPhysChem* **2000**, *1*, 18. (b) Rivas, L.; Sanchez-Cortes, S.; Garcia-Ramos, J. V.; Morcillo, G. *Langmuir* **2000**, *16*, 9722. (c) Mallik, K.; Mandal, M.; Pradhan, N.; Pal, T. *Nano Lett.* **2001**, *1*, 319.
- (7) Chen, Y.-H.; Yeh, C.-S. *Chem. Commun.* **2001**, 371.
- (8) (a) Papavassiliou, G. C. *J. Phys. F* **1976**, *6*, L103. (b) Link, S.; Wang, Z. L.; El-Sayed, M. A. *J. Phys. Chem. B* **1999**, *103*, 3529.
- (9) (a) Sibbald, M. S.; Chumanov, G.; Cotton, T. M. *J. Phys. Chem.* **1996**, *100*, 4672. (b) Mafune, F.; Kohno, J.; Takeda, Y.; Kondow, T.; Sawabe, H. *J. Phys. Chem. B* **2000**, *104*, 8333. (c) Brause, R.; Möltgen, H.; Kleinermanns, K. *Appl. Phys. B* **2002**, *75*, 711.
- (10) Lee, I.; Han, S. W.; Kim, K. *Chem. Commun.* **2001**, 1782.
- (11) (a) El-Sayed, M. A. *Acc. Chem. Res.* **2001**, *34*, 257. (b) Kamat, P. V. *J. Phys. Chem. B* **2002**, *106*, 7729.
- (12) Peng, Z.; Walther, T.; Kleinermanns, K. *Langmuir* **2005**, *21*, 4249.
- (13) (a) Last, I.; Schek, I.; Jortner, J. *J. Chem. Phys.* **1997**, *107*, 6685. (b) Kamat, P. V.; Flumiani, M.; Hartland, G. V. *J. Phys. Chem. B* **1998**, *102*, 3123.
- (14) Shibata, T.; Bunker, B. A.; Zhang, Z.; Meisel, D.; Vardeman, C. F., II; Gezelter, J. D. *J. Am. Chem. Soc.* **2002**, *124*, 11989.
- (15) (a) Evanoff, D. D., Jr.; Chumanov, G. *J. Phys. Chem. B* **2004**, *108*, 13957. (b) Evanoff, D. D., Jr.; Chumanov, G. *ChemPhysChem* **2005**, *6*, 1221.
- (16) Inasawa, S.; Sugiyama, M.; Yamaguchi, Y. *J. Phys. Chem. B* **2005**, *109*, 9404.
- (17) Dawson, A.; Kamat, P. V. *J. Phys. Chem. B* **2001**, *105*, 960.
- (18) Mafune, F.; Kohno, J.; Takeda, Y.; Kondow, T. *J. Phys. Chem. B* **2002**, *106*, 8555.
- (19) Mafuné, F.; Kohno, J.; Takeda, Y.; Kondow, T. *J. Phys. Chem. B* **2003**, *107*, 12589.
- (20) Peng, Z.; Walther, T.; Kleinermanns, K. *J. Phys. Chem. B* **2005**, *109*, 15735.